*Biology of Reproduction*, 2018, 98(1), 102–114
doi:10.1093/biolre/iox150
Research Article
Advance Access Publication Date: 17 November 2017

Research Article

# Nuclear localization of EIF4G3 suggests a role for the XY body in translational regulation during spermatogenesis in mice†

**Jianjun Hu‡, Fengyun Sun‡ and Mary Ann Handel***

The Jackson Laboratory, Bar Harbor, Maine, USA

***Correspondence:** The Jackson Laboratory, 600 Main Street, Bar Harbor, ME 04609, USA. Tel: +207-288-6778; E-mail: maryann.handel@jax.org

†**Grant Support:** This work was supported by the NIH, HD73077 to MAH and P30 CA034196 to the Jackson Laboratory for scientific services; the content is solely the responsibility of the authors and does not necessarily represent official views of the NIH.

‡These authors contributed equally.

Edited by Dr. Monika A. Ward, PhD, University of Hawaii John A. Burns School of Medicine.

Received 26 July 2017; Revised 25 October 2017; Accepted 16 November 2017

## ABSTRACT

Eukaryotic translation initiation factor 4G (EIF4G) is an important scaffold protein in the translation initiation complex. In mice, mutation of the *Eif4g3* gene causes male infertility, with arrest of meiosis at the end of meiotic prophase. This study documents features of the developmental expression and subcellular localization of EIF4G3 that might contribute to its highly specific role in meiosis and spermatogenesis. Quite unexpectedly, EIF4G3 is located in the nucleus of spermatocytes, where it is highly enriched in the XY body, the chromatin domain formed by the transcriptionally inactive sex chromosomes. Moreover, many other, but not all, translation-related proteins are also localized in the XY body. These unanticipated observations implicate roles for the XY body in controlling mRNA metabolism and/or "poising" protein translation complexes before the meiotic division phase in spermatocytes.

### Summary Sentence

In spermatocytes, translation initiation factor EIF4G3 localizes almost exclusively to the XY body, suggesting a role for this chromatin domain in post-transcriptional regulation of spermatogenic gene expression.

**Key words:** translational regulation, meiosis, spermatocyte, nucleus, sex chromosomes.

## Introduction

Mammalian spermatogenesis is an integrated and specialized process of differentiation that is reflected in the complexity of the testicular transcriptome and germ-cell strategies for post-transcriptional regulation of translation [1–4]. Spermatogenesis encompasses stem-cell specification, mitotic proliferation of spermatogonia, the prolonged prophase of meiosis, and postmeiotic spermiogenic differentiation of mature spermatids. The cell biology of spermatogenesis dictates the necessity of post-transcriptional and translational-level regulation because the spermatid nucleus is condensed and transcriptionally inactivated before the need for new protein ceases. Many transcripts, such as those for protamines, are synthesized during meiotic prophase or in round spermatids immediately after the meiotic divisions, and stored for days before translation [5,6]. Thus, there must be tight regulation of RNA-binding proteins (RBPs) and the RNA recognition sequences [6,7], and likewise regulation of their cellular compartmentalization.

Timely translation is a mechanism for prompting steps of spermatogenic differentiation, including progress from meiotic prophase to the division phase. During the temporally extended meiotic prophase, important genetic events include homology-based pairing

of chromosomes and reciprocal recombination events resulting in crossovers, which are essential for ensuring accurate segregation of chromosomes during the meiotic divisions [8]. The end of meiotic prophase and entry into the meiotic division phase (the G2/MI transition) is executed by multiple kinases [9–12]. One of the most important of these is MPF, the metaphase-promoting factor complex, which is activated in part by the heat-shock protein 2 (HSPA2) [13,14]. However, exactly how all of these meiotic G2/MI transition events are signaled and coordinated is not yet fully understood, although evidence suggests that there is temporal regulation by translational control. For example, in the fruit fly *Drosophila*, the translation initiation complex factor eIF4G2 coordinates spermatogenesis by controlling cell-cycle progress [15,16], and in *Caenorhabditis elegans*, the translation factor ife-1 controls meiotic division [17,18], as well as events of earlier meiotic prophase [19].

We have previously demonstrated a genetic requirement for the eukaryotic translation initiation factor EIF4G3 for onset of the meiotic division phase of spermatogenesis in mice [20]. In mice, there are three EIF4G proteins: the canonical and ubiquitously abundant EIF4G1, and EIF4G2 and EIF4G3. Although EIF4G3 is ubiquitously expressed, mutation of the *Eif4g3* gene, by either of two gene-trap mutations or by the single base-pair *Eif4g3*$^{repro8}$ mutation, results in male infertility, but no other obvious phenotypes [20]. Thus, EIF4G3 has specific function in spermatogenesis. Consistent with the canonical role of EIF4G3 in translation initiation, we previously identified *Hspa2*, encoding the heat-shock chaperone protein HSPA2, as a likely substrate of EIF4G3, because its translation is blocked by mutation of the *Eif4g3* gene [20]. The depletion of HSPA2 protein may explain much or all of the *Eif4g3*$^{repro8}$ mutant testis phenotype of germ-cell arrest at the end of meiotic prophase, given that HSPA2 is required for activation of MPF, thus promoting the transition to the division phase [13,14].

EIF4G3 is part of the eukaryotic translation initiation 4F (EIF4F) complex, which is a conserved and ubiquitous mRNA cap-binding complex. It mediates the first, rate-limiting, step of translation initiation by assembling on the 7-methylguanosine cap structure of mRNAs. EIF4F is composed of three proteins: the cap-binding protein eukaryotic translation initiation factor 4E (EIF4E), the scaffolding protein EIF4G, and the ATP-dependent RNA helicase eukaryotic translation initiation factor 4A (EIF4A). Assembly of the complex facilitates the formation of a mRNA "closed loop" by interacting with poly(A)-binding protein (PABP) as well as with the 5′ cap. This complex accomplishes unwinding of local secondary structure in the 5′ untranslated region of the mRNA substrate, recruits additional translation factors and the small 40S ribosomal subunit, and ultimately is replaced on the mRNA by the translation elongation complex. In addition to the role of EIF4G in translation initiation, alternative roles for this protein have recently been proposed, including nuclear mRNA biogenesis and surveillance [21].

We have studied features of the developmental expression and subcellular localization of EIF4G3 that might contribute to its highly specific role in meiosis and spermatogenesis. Unexpectedly, we find that in the critical time frame of its function, EIF4G3 and other protein translation proteins are specifically localized in the XY body of the meiotic spermatocyte nucleus. The XY (or sex) body is a chromatin domain formed by the transcriptionally inactive sex chromosomes, which are paired only in their short region of shared homology and are transcriptionally inactivated [22,23]. Our observations on EIF4G3 localization implicate a role for the XY body in controlling mRNA metabolism and/or protein translation leading to the meiotic cell-cycle transition in spermatocytes.

## Materials and methods

### Animals

The *repro8* mutation of *Eif4g3* was induced on the C57BL/6J (B6) background, outcrossed to C3HeB/FeJ (C3H) as previously reported [20], and a congenic line on C3H was created. All *Eif4g3*$^{repro8}$ mice and control littermates used for the current biological analyses were from the congenic line. The *repro8* mutation is a single base change in the last exon, producing an ala-pro amino acid change [20]; this site was verified by PCR using the following primers: forward: 5′-TGT TGT CAC CTC TTG CAG ACT T- 3′; reverse, 5′-TTG TTT CTT TTG TTT CGT TTG TG-3′ and followed by allele sequencing with the forward primer. The *Eif4g3* exon 5-specific conditional knockout mice (B6(Cg)-*Eif4g3*$^{tm1.2Hand}$/Hand) were made by Genetic Engineering Technologies (GET) at The Jackson Laboratory following standardized methods. In brief, pUC57-Simple vector was used for exon 5 targeting. The total size of the targeting vector was 18,749 bp, and the short and long homology arms were 4959 bp and 6940 bp, respectively. The distance between the 5′ LoxP and the 3′PGKNEO cassette is 458 bp. The 5′ LoxP site is 319 bp to exon 5 and the PGKNEO cassette is 105 bp away from exon 5. The vector was linearized with Asc1 for targeting C57BL/6N JM8A3 ES cells. The chimeras were crossed with B6N.129-GT(ROSA)26Sor$^{tm1(FLP1)Dym}$/J to test for germline transmission and excise PGKNEO cassette. Mice with germline transmission were then crossed with ubiquitous *Sox2*-cre mice to produce offspring with the exon-5 deleted allele. PCR was used for genotyping. PCR primers for the conditional-ready mice were as follows: forward, 5′-TTG GTT TCT GTT GCG TTT CTG ACT C-3′, and reverse, 5′-TGA AAC TAA CAA GAA GTA AAG CCA AGC-3′. PCR primers for exon-5-deleted mice were as follows: forward primer (common primer for wild type allele and exon-5 deleted allele), 5′-TTT ATA GTG TAA CCA CTT CTG GTG-3′; reverse primer for wild type allele, 5′-GAT GAT GGG CAG GTC GAG-3′; reverse primer for exon-5 deleted allele, 5′-TGA AAC TAA CAA GAA GTA AAG CCA AGC-3′. The B6.129 × 1-*Spo11*$^{tm1Mjn}$/J mice were obtained from The Jackson Laboratory and maintained by heterozygous breeding. The following primers were used for genotyping: wild-type forward, 5′-TCA GGA CAG GGC ATA GCA GT-3′; mutant forward, 5′- GCC AGA GGC CAC TTG TGT AG-3′, and common reverse, 5′-CTG CTC AGG GAG GAG AAC AC-3′ (mutant = ∼340 bp, heterozygote = 165 bp and ∼340 bp, wild type = 165 bp). Approximately 14 dpp heterozygous and homozygous *Spo11*$^{tm1Mjn}$/J testes were used for germ-cell isolation and immunofluorescence staining. All mice were maintained following protocols approved by the Jackson Laboratory (JAX) Institutional Animal Care and Use Committee, and experiments were conducted in accordance with specific guidelines and standards of the Society for the Study of Reproduction.

### Germ-cell isolation and enrichment

Mice at appropriate ages were killed by cervical dislocation. For direct germ-cell isolation, testes were removed, detunicated, and digested in DMEM containing Liberase (cat. #10569-010, Gibco) at 32°C for 20 min, followed by a second digestion at 32°C for 13 min after washing with serum-free DMEM. After digestion, the cell suspension was filtered through an 80-$\mu$m mesh filter and washed two times in DMEM and one time in 1× PBS. For enrichment of pachytene/diplotene spermatocytes and round and elongated spermatids, germ cells were isolated with Krebs-Ringer bicarbonate solution (KRB) (120.1 mM NaCl, 4.8 mM KCl, 25.2 mM $NaHCO_3$,

1.2 mM $KH_2PO_4$, 1.2 mM $MgSO_4.7H_2O$, 1.3 mM $CaCl_2$, 11 mM glucose, 1× essential amino acids, 1× nonessential amino acids) at 32°C for 20 min, followed by digestion in KRB containing 0.5 mg/ml trypsin (Sigma) and 20 mg/ml DNase I at 32°C for 13 min. Crude germ cells were further loaded into the STA-PUT sedimentation system. Pachytene/diplotene spermatocytes and round spermatids were enriched by velocity sedimentation as previously described [24]. Isolated germ cells were then processed for immunofluorescence staining as described below.

### Histology and immunohistochemistry

Testes were fixed in Bouin's solution in PBS or 4% paraformaldehyde (PFA) plus 2% trichloroacetic acid in 0.9% saline overnight, paraffin-embedded, sectioned (5 $\mu$m) and stained with periodic acid Schiff. For immunohistochemistry, sections were blocked with 5% bovine serum album in PBS at room temperature for 30 min. Primary antibodies (Table 1) were applied and slides were incubated at 37°C for 1 h. Antigens were localized using SuperPicTure Polymer Detection Kit (Zymed/Invitrogen, South San Francisco, CA, USA), sections were counterstained with hematoxylin (Sigma Aldrich, St Louis, MO, USA), and then mounted in ClearMount (Zymed/Invitrogen). Images were acquired with a NanoZoomer 2.0HT, model #C9600–12 microscope (Hamamatsu, Japan).

### Surface-spread chromatin, whole-mount and immunofluorescence staining

Spermatocytes isolated as described above were collected by centrifugation, surface-spread in wells of multispot slides (Shandon, Pittsburgh, PA, USA) and fixed as previously described [11,25,26]. Spermatocytes for whole-mount preparations were placed on poly-L-lysine precoated slides for 30 min, fixed with 4% PFA for 30 min and followed by 0.3% Triton X-100 permeabilization for 15 min. All samples were blocked with 5% bovine serum album for 30 min. Primary antibodies were diluted in 5% bovine serum album and used as shown in Table 1. Secondary antibodies conjugated with Alexa Fluor 594 or 488 (Molecular Probes, Invitrogen, Carlsbad, CA, USA) were used at 1:500 dilution. Images were acquired with Zeiss Axio Imager Z2 or Leica SP5 confocal microscopes. The HEK293 cells growing on cover slips were fixed with 2% PFA after a brief wash and treated with 0.3% Triton X-100/PBS for 10 min. Cells were then stained with EIF4G3 antibody (Bethyl) following the standard immunofluorescence staining protocol.

### Puromycin assay for protein synthesis

For in situ analysis of ongoing protein synthesis, the method of puromycin incorporation was used [27,28]. The principle of this localization analysis is based on ribosome-catalyzed puromycylation of nascent peptide chains following incorporation of puromycin and immobilization on ribosomes by treatment with a chain-elongation inhibitor (Emetine). The sites of puromycin incorporation are visualized with a puromycin-specific monoclonal antibody in fixed and permeabilized cells. These assays were performed on spermatocytes enriched by separation on a STA-PUT BSA gradient as described above. For each group, $1 \times 10^6$ germ cells were suspended in 1 ml MEM alpha containing 5% fetal bovine serum, lactic acid, HEPES and 1x antibiotics [24] in four-well plates and incubated for 1 h. Subsequently, 5 $\mu$M puromycin (Cat. #P8833, Sigma; dissolved in ethanol) and ethanol control with 200 $\mu$M emetine (Cat. #E2375, Sigma; dissolved in ethanol) were added to the medium and cells were incubated for 5 min. Treated germ cells were collected briefly by centrifugation at 100 *g* for 3 min and washed once with PBS. After surface spreading or whole-mount preparation, germ cells were stained with a monoclonal antibody recognizing puromycin.

### RNA extraction and quantitative RT-PCR

Total RNA was isolated from whole testes using the RNeasy Mini Kit (Qiagen, Valencia, CA, USA) and 1 $\mu$g RNA was reverse transcribed using QuantiTect Reverse Transcription Kit (Qiagen), according to the manufacturer's instructions. Quantitative RT-PCR (qRT-PCR) was performed on the Applied Biosystems 7500 Real-Time PCR System (Applied Biosystems, Foster City, CA) using the QuantiTect SYBR Green® RT-PCR kit (Qiagen). Gene-specific primers were used to determine the overall relative expression levels of *Eif4g1, Eif4g3, Dazl, Elavl1, and Pabpc1,* according to the standard curve method [29]. Primers were designed to span introns and amplify all known transcript variants of the genes. Quantitative RT-PCR results were normalized to their corresponding glyceraldehyde-3-phosphate dehydrogenase (Gapdh) content. The following primers were used: for *Eif4g1*, forward: 5′-CTG GAC AAG GCC AAT AAA ACA-3′ and reverse: 5′-GTT TCC AAG CCT TCT CTG CTT-3′; for *Eif4g3*, forward: 5′-GAT GCA GGA CAA AGC AGA GTC-3′ and reverse: 5′-TAA CAC TTC ATC TGG GGT TCG-3′; for *Dazl*, forward: 5′-ATG TCT GCC ACA ACT TCT GAG-3′ and reverse: 5′-CTG ATT TCG GTT TCA TCC ATC CT-3′; for *Elavl1*, forward: 5′-TGT CCT GCT ACT TTA TCC CGA-3′ and reverse: 5′-GGA TGA CAT TGG GAG AAC GAA T-3′; for *Pabpc1*, forward: 5′-CAA GCC AGT ACG CAT CAT GTG-3′ and reverse: 5′-TGC TTC CTG TGT TTC AAA GTG T-3′; for *Gapdh*, forward: 5′-AGG TCG GTG TGA ACG GAT TTG-3′ and reverse: 5′-TGT AGA CCA TGT AGT TGA GGT CA-3′.

### Western blot analyses

Total protein was extracted from testes using the RIPA buffer (Santa Cruz, Santa Cruz, CA, USA) containing protease inhibitor cocktail (Santa Cruz). Protein concentration was measured by the BCA method (Pierce Biotechnology, Rockford, IL, USA). Protein (20 $\mu$g) from each group was boiled for 5 min, and proteins were separated by electrophoresis using precast 4%–15% SDS-PAGE (Bio-Rad, Hercules, CA, USA). Proteins were transferred onto PVDF membranes (Millipore, Temecula, CA, USA). The membranes were blocked overnight at 4°C with 5% dried milk in Tris-buffered saline with 0.1% Tween-20, and then probed with antibodies at concentrations specified in Table 1. The blots were incubated for 1 h with primary antibody at room temperature, and then incubated with horseradish peroxidase-conjugated secondary antibodies made from mouse or rabbit (Invitrogen, South San Francisco, CA, USA) for 45 min at room temperature. Proteins were detected using Pierce ECL Plus Western Blotting substrate (Thermo Scientific, IL, USA).

### Protein interactions

Co-immunoprecipitation (co-IP) was performed using the Dynabeads Coimmunoprecipitation Kit (Invitrogen, Carlsbad, CA, USA), according to the manufacturer's instructions. Briefly, the antibody coupling reaction was performed by incubating 5 mg beads and 35 $\mu$g antibody (7 $\mu$g/mg beads) or IgG (as a control) for 18 h at 37°C. After washing, the antibody-coupled beads were resuspended in SB buffer at a concentration of 10 mg/ml and stored at 4°C. Protein was extracted from whole testes with extraction buffer containing protease inhibitors at a 1:9 ratio of tissue sample to extraction buffer. Protein concentration was measured by the BCA

**Table 1.** Primary antibodies used in this study.

| | | | | | Dilution | |
|---|---|---|---|---|---|---|
| Antibody | Host | Producer | Cat. # | RRID | IF/IHC | WB |
| EIF4G1 | Rab | Cell signaling | 8701S | AB_11178378 | 1:100 | 1:3000 |
| EIF4G2 | Rab | Cell signaling | 5169S | AB_10622189 | 1:100 | n/a |
| EIF4G3 | Rab | Bethyl | A301–769A | AB_1211018 | 1:100 | n/a |
| EIF4G3 | Rab | Thermo | PA5–31101 | AB_2548575 | n/a | 1:3000 |
| EIF4G3-exon5 | Rab | HandelLab/ Thermo | n.a. | n.a. | 1:100 | n.a |
| EIF4E | Mo | Thermo | MA1–089 | AB_2536738 | 1:100 | 1:2000 |
| EIF4E2 | Mo | Santa Cruz | sc-100731 | AB_1122491 | 1:100 | n/a |
| EIF4E3 | Rab | ProteinTech | 17282–1-AP | AB_2262162 | 1:100 | n/a |
| EIF4A1 | Mo | Thermo | MA5–14901 | AB_11006110 | 1:100 | n/a |
| EIF4A2 | Rab | ProteinTech | 11280–1-AP | AB_2097378 | 1:100 | 1:2000 |
| EIF4A3 | Rab | Abcam | Ab32485 | AB_732124 | 1:50 | n/a |
| SYCP3 | Rat | Handel Lab. | Eaker et al.,2001 | n.a. | 1:500 | n/a |
| pH2AFX | Mou | Millipore | 05–636 | AB_309864 | 1:200 | n/a |
| ATR | Go | Santa Cruz | sc-1887 | AB_630893 | 1:50 | n/a |
| HIST1H1T | G. Pig | Handel Lab. | Cobb et al.,1999 | n.a. | 1:500 | n/a |
| POLR2A | Mo | Abcam | Ab32485 | AB_732124 | 1:100 | n/a |
| RPS3 | Rab | Thermo | PA5-27974 | AB_2545450 | 1:100 | n/a |
| RPS6 | Mo | Thermo | MA5-15123 | AB_10999800 | 1:100 | n/a |
| RPS13 | Rab | Abcam | Ab104862 | AB_10712319 | 1:100 | n/a |
| RPL10A | Mo | Santa Cruz | sc-100827 | AB_2285311 | 1:100 | n/a |
| RPL10L | Mo | Abnova | 115–214 | AB_10864171 | 1:50 | n/a |
| RPL28 | Go | Santa Cruz | sc-14151 | AB_2181749 | 1:100 | n/a |
| EIF4EBP1 | Go | Santa Cruz | sc-6025 | AB_633426 | 1:100 | n/a |
| AGO4 | Go | Santa Cruz | sc-32664 | AB_2277670 | 1:100 | n/a |
| MKNK1 | Rab | Cell Signaling | 2195S | AB_2235175 | 1:100 | n/a |
| MKNK2 | Rab | Abcam | Ab84345 | AB_1860814 | 1:100 | n/a |
| PABPC1 | Rab | Abcam | Ab21060 | AB_777008 | 1:100 | 1:1000 |
| BOLL | Rab | Thermo | PA5-30808 | AB_2548282 | 1:150 | n/a |
| DAZL | Rab | Cell signaling | 8042S | AB_10860078 | 1:150 | 1:2000 |
| ELAVL1 | Rab | Millipore | 07-468 | AB_310641 | 1:200 | 1:2000 |
| MSI1 | Go | R&D | AF2628 | AB_2147926 | 1:50 | n/a |
| TSN | Rab | Abcam | Ab71775 | AB_1524509 | 1:50 | n/a |
| HSPA2 | Rab | ProteinTech | 12797-1-AP | AB_2119687 | 1:500 | n/a |
| pCDK1 | Rab | Thermo | MA5-15062 | AB_10984869 | 1:50 | n/a |
| pCDK2 | Rab | Cell signaling | 2561S | AB_2078685 | 1:100 | n/a |
| pCHEK1 | Rab | Cell signaling | 2341S | AB_330023 | 1:100 | n/a |
| pCHEK2 | Rab | Abcam | Ab59408 | AB_942224 | 1:100 | n/a |
| p4EBP1(S64) | Rab | Cell Signaling | 9451S | AB_330947 | 1:100 | n/a |
| p4EBP1(T69) | Rab | Cell Signaling | 9455S | AB_330949 | 1:50 | n/a |
| p4EBP1(S111) | Rab | Abgent | AP3473a | AB_1278020 | 1:50 | n/a |
| Puromycin | Mo | Millipore | MABE343 | AB_2566826 | 1:10 000 | n/a |
| TUBA1A | Mo | Sigma | T9026 | AB_477593 | 1:500 | 1:5000 |
| TUBG1 | Go | Santa Cruz | sc-7396 | AB_2211262 | 1:200 | n/a |
| FLAG | Mo | Sigma | F1804 | AB_262044 | 1:200 | n/a |

method (Pierce Biotechnology). 1.5 mg coupled Dynabeads were used for immunoprecipitation. Immunoprecipitation was carried out for 20 min at 4°C under rotation, followed by elution of precipitated protein with 2X Laemmli buffer at 100°C for 10 min. The eluting complex was subjected to SDS-PAGE separation for western blotting as above. The antibodies used are listed in Table 1.

Testis tissue used for isolation of the mRNA cap-binding protein complex was lysed in buffer containing 50 mM Hepes, pH 7.4, 75 mM NaCl, 10 mM $MgCl_2$, 1 mM DTT, 8 mM EGTA, 10 mM $\beta$-glycerophosphate, 0.5 mM $Na_3VO_4$, 0.5% Triton X-100, and protease inhibitor cocktail. Cell extracts were incubated for 10 min on ice and centrifuged at 12,000 *g* for 10 min at 4°C. The supernatants were precleared for 1 h on Sepharose beads (Cat #20182006-1, BioWorld). After centrifugation for 1 min at 1000 *g*, supernatants were recovered and incubated for 2 h at 4°C with $\gamma$-aminophenyl m7GTP –Sepharose or control Sepharose (Jena Bioscience) under constant shaking. Beads were washed three times with lysis buffer, and absorbed proteins were eluted in SDS-PAGE sample buffer.

## Cell culture, plasmid construction, and transfection

HEK293 cells were cultured with high glucose DMEM (cat. #10569, Gibco), containing 10% FBS (cat. #DE14-801FH, Lonza), antibiotics mix 100 IU/ml penicillin and 100 $\mu$g/ml streptomycin (cat. #15140-122, Gibco). For transfection, Lipofectamine 2000 (cat. #11668-019, Invitrogen) was used as recommended by the

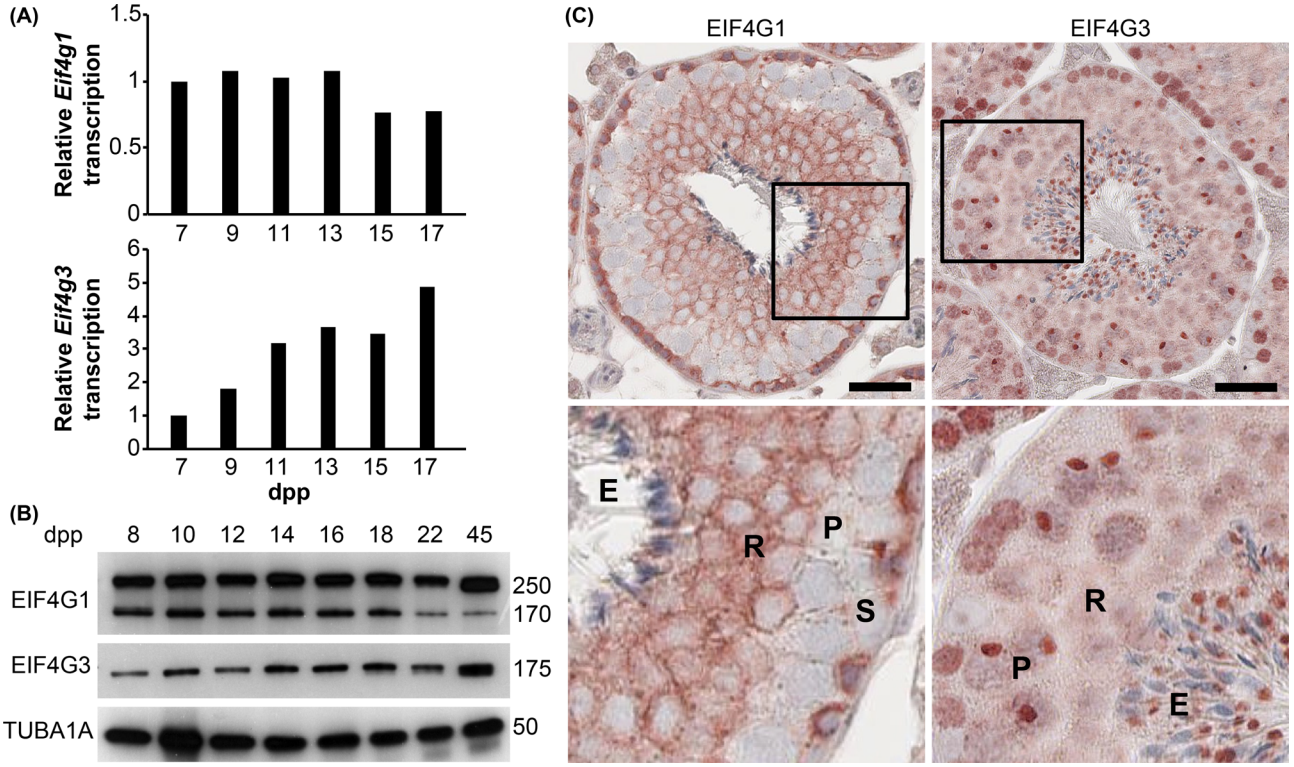


**Figure 1.** Expression of *Eif4g1* and *Eif4g3* and their cellular localization during spermatogenesis. (**A**) Quantitative RT-PCR analysis of mRNA levels of *Eif4g1* and *Eif4g3* in testes from 7 to 17 dpp. Each analysis was performed twice, and representative results are shown. *Gapdh* was used as an internal control. (**B**) Western-blot analysis of protein levels of EIF4G1 and EIF4G3 in testis during the first wave of spermatogenesis. Total protein extracts were prepared from whole testes of mice at age of 8–45 dpp. The loading control is TUBA1A; position of molecular weight markers (kDa) is shown to the right. (**C**) The top two panels show immunohistochemical labeling of EIF4G1 and EIF4G3 of seminiferous tubule cross sections, with boxed area in higher magnification in the lower two panels, showing details of cellular localization of EIF4G1 and EIF4G3. E = elongating spermatids; R = round spermatids; P = pachytene spermatocytes, S = spermatogonia. Bars = 40 $\mu$m.

manufacturer. The *Eif4g3* ORF obtained from OriGene (Cat #MC206135, Origene, RefSeq: BC072600) was used as the template for PCR. This was cloned into EGFP-N1 vector (Clontech) with a linker sequence to ensure that the downstream EGFP was in-frame with *Eif4g3*. *Eif4g3* was also amplified by PCR and inserted into the pCMV-3xFLAG vector for expression of EIF4G3-FLAG. Purified plasmids were transfected into HEK293 cells separately. Twenty-four hours after transfection, the cells were passaged and seeded onto sterile poly-L-lysine coated cover slips and were further cultured overnight.

## Results

### EIF4G1 and EIF4G3 are differentially expressed in germ cells during spermatogenesis

We first determined that both EIF4G1 (the canonical initiation scaffolding factor) and EIF4G3 are expressed in male germ cells throughout spermatogenesis. The respective mRNAs and proteins are both expressed during prepubertal and pubertal development (Figure 1). The *Eif4g1* transcript exhibited downregulation with developmental age, while *Eif4g3* increased throughout early development (Figure 1A). Similar transcription patterns for *Eif4g1* and *Eif4g3* were also observed in our RNA-seq data profiled with purified germ cells at different developmental stages [3]. This developmental pattern was confirmed by western blotting of testes (Figure 1B). Immunohistochemical staining of testis sections from adult males demonstrated that both EIF4G1 and EIF4G3 were expressed in germ cells throughout spermatogenesis, from spermatogonial stages to mature spermatids (Figure 1C). However, the two translation initiation factors differed in both developmental pattern and cellular specificity of protein expression. The canonical EIF4G1 was most abundant in very early prophase spermatocytes and spermatids, but diminished in pachytene and diplotene spermatocytes. In contrast, EIF4G3 was most abundant in the mid-to-late prophase spermatocytes, and also present in elongating spermatids. Notably, the subcellular localization of the two proteins differed dramatically. EIF4G1 exhibited predominantly cytoplasmic localization in all germ cells, while in contrast, EIF4G3 exhibited nuclear localization in meiotic prophase spermatocytes (Figure 1C), a point addressed in more detail below. Together, these observations suggest differential function of EIF4G1 and EIF4G3 during meiotic prophase, consistent with the meiotic arrest phenotype of *Eif4g3* mutants [20].

### EIF4G3 is present in EIF4F translation initiation complexes and interacts with RNA-binding proteins

EIF4G is an integral component of the EIF4F translation initiation complex in somatic cells. We determined whether EIF4G3 interacts with EIF4F complex proteins in lysates of testes from mice at 14 dpp (a time when the germ-cell composition of mutant and wild-type testes is similar). We first used an mRNA cap analog, immobilized $\gamma$-aminophenyl m7GTP, to precipitate the EIF4F complex from the

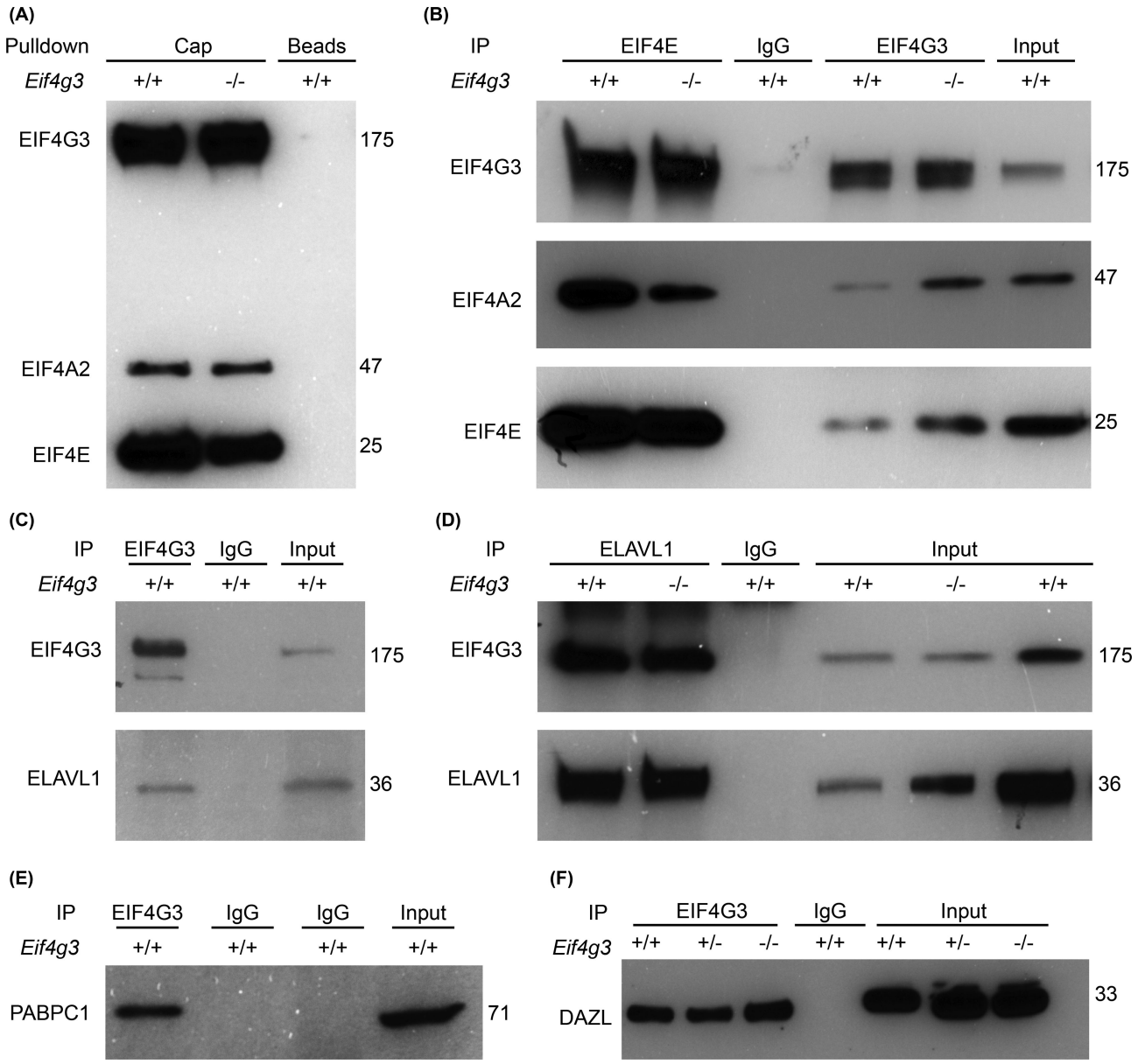


**Figure 2.** Cap-analog pull-down and co-immunoprecipitation (Co-IP) analyses of interaction of EIF4G3 with other proteins. (**A**) Cap-analog pull-down analysis with whole testis protein extracts from adult wild-type (+/+) and *Eif4g3*$^{repro8/repro8}$ mutant (–/–) mice. The $\gamma$-aminophenyl m7GTP cap analog was used as bait to pull-down cap-binding protein complexes. Sepharose 4B was used as a negative control. The pull-down samples were analyzed by western blotting with mixture of EIF4G3, EIF4A2 and EIF4E antibodies. (**B**) Co-IP using anti-EIF4E and anti-EIF4G3 antibodies with whole testis protein extracts from adult wild-type (+/+) and *Eif4g3*$^{repro8/repro8}$ mutant (–/–) mice followed by western blot analysis with EIF4G3, EIF4A2, and EIF4E antibodies. (**C-D**) Reciprocal co-IP using EIF4G3 (**C**) and ELAVL1 (**D**) antibodies with whole testis protein extracts from adult wild-type (+/+, at two concentrations) and *Eif4g3*$^{repro8/repro8}$ (–/–) mutant mice, followed by western blot analysis with EIF4G3 and ELAVL1 antibodies. (**E**) IP analysis using anti-EIF4G3 antibody for immunoprecipitation from testis extracts of adult wild type (+/+), followed by western blotting with anti-PABPC1. (**F**) IP analysis using anti-EIF4G3 antibody for immunoprecipitation from testis extracts of adult wild-type (+/+), *Eif4g3*$^{repro8/repro8}$ mutant (–/–) and heterozygous (+/–) mice, followed by western blotting with DAZL antibody. Molecular weights (kDa), inferred from markers co-electrophoresed, are shown to the right of each blot.

testis lysates [30], and determined the presence of EIF4G3 by western blotting. As shown in Figure 2A, EIF4G3 was detected in the pull down of the 14 dpp testis extract; moreover, both EIF4E and EIF4A2 (two other integral components of the EIF4F complex) were also detected in the same fraction. To further test these interactions among the complex members, we carried out reciprocal co-IP with EIF4G3 and EIF4E antibodies. As shown in Figure 2B, when EIF4E antibody was used for immunoprecipitation, both EIF4G3 and EIF4A2 were detected, and when EIF4G3 antibody was used for immunoprecipitation, both EIF4A2 and EIF4E were co-immunoprecipitated. These observations demonstrate that EIF4G3 interacts with components of EIF4F complex in testis lysates, suggesting its engagement in cap-dependent translation in the testis. Moreover, these components of the EIF4F complex were also detected in *Eif4g3*$^{repro8}$ mutant testes (Figure 2B), indicating their accumulation is not dependent on the mutated C-terminal domain of EIF4G3.

Translation initiation complexes interact with RBPs to form ribonucleoprotein complexes. RBPs influence the structure of RNAs and play critical roles in RNA biology, including mRNA translation, and thus could be key to understanding the translational specificity of EIF4G3 in testes. We confirmed expression of different RBPs known to be required or expressed during spermatogenesis, including deleted in azoospermia-like (DAZL) [31], ELAV (embryonic lethal, abnormal vision)-like 1(ELAVL1) [32], and poly(A) binding protein, cytoplasmic 1 (PABPC1) [33], at transcriptional and translational levels, during the first wave of spermatogenesis from 8 to 35 dpp (Supplementary Figure S1). Expression of DAZL and ELAVL1 peaked at 18–21 dpp, which is when mid-to-late pachytene spermatocytes are abundant in the testis, and also when spermatogenesis in *Eif4g3*$^{repro8}$ mutant testes is arrested (Supplementary Figure S1A and B). Immunohistochemistry analysis revealed differential localization of RBPs in spermatocytes, with DAZL and PABPC1 being predominantly cytoplasmic, and ELAVL1 being nuclear (Supplementary Figure S1C). Western blotting of protein precipitated by anti-EIF4G3 revealed the presence of ELAVL1 (Figure 2C), PABC1 (Figure 2E), and DAZL (Figure 2F) in the immunoprecipitates, and immunoprecipitation with anti-ELAVL1 antibody co-immunoprecipitated EIF4G3 (Figure 2D). These interactions were also observed in the immunoprecipitation experiment using protein extract from *Eif4g3*$^{repro8}$ mutant testes (Figure 2D and F), suggesting that even the mutant EIF4G3 protein can interact with these RBPs.

## EIF4G3 localizes to the XY body of pachytene spermatocyte nuclei

Because the nuclear localization of EIF4G3 was unexpected, we characterized it using a wide variety of cytological preparation methods and antibodies to avoid misinterpretation based on possible artifact. Due to the lack of a complete *Eif4g3* knockout for validating antibody, we tested the specificity of the EIF4G3 antibody by expressing EIF4G3 with EGFP or FLAG tags in HEK293 cells. In this expression system, the EIF4G3 protein tag signals co-localized with anti-EIF4G3 antibody signal (Supplementary Figure S2), providing validation for the antibody. In both spread chromatin and nuclear whole-mount preparations, EIF4G3 was detected in spermatocyte nuclei, especially those immunolabeled for characteristic pachytene-stage marker proteins, such as synaptonemal complex protein 3 (SYCP3) (Figure 3A; Supplementary Figure S3). In contrast, the canonical EIF4G1 was not detected in spermatocyte nuclei (Figure 3B; Supplementary Figure S3A). Although nuclear localization of EIF4G3 was most prominent in pachytene spermatocytes, it was also detected in leptotene and zygotene spermatocytes (Figures 1C and 3A). Interestingly, although there was relatively weaker expression of EIF4G3 in round spermatids, there was a dramatic increase in expression in elongating spermatids, where it is located in the cytoplasmic region (Figure 1).

The subnuclear localization of EIF4G3 in pachytene spermatocyte nuclei was almost exclusively to the XY body, the domain containing the largely unpaired and transcriptionally inactive sex chromosomes [22,23]. EIF4G3 localization specifically to the XY body appeared to be from mid to late pachynema, as it is found most robustly in histone cluster 1, H1t (HIST1H1T)-positive cells, but not in HIST1H1T-negative cells (Figure 3C); HIST1H1T is a marker of mid-pachynema [9,34]. The specificity of this localization was confirmed using common diagnostic markers of the XY body, particularly phosphorylated H2A histone family, member X (pH2AFX). In both spread chromatin and whole-mount preparations, EIF4G3 (but not EIF4G1) co-localized with pH2AFX in pachytene spermatocytes (Figure 3D). Likewise, we found EIF4G3 co-localized with ATR (ataxia telangiectasia and Rad3 related, a kinase involved in meiotic DNA repair), another marker of the XY body (Figure 3D), but not with HIST1H1T (histone H1t) or polymerase (RNA) II (DNA directed) polypeptide A (POLR2A) (RNA polymerase 2A), which do not localize to the XY body and are markers of the autosomal chromatin domain of pachytene spermatocyte nuclei (Figure 3C and E). Finally, localization of EIF4G3 in pachytene spermatocytes was not enriched with protein markers of the cytoplasm (detected best in whole-mount preparations), such as the mRNA processing P-body protein piwi-like RNA-mediated gene silencing 2 (PIWIL2) (Supplementary Figure S3C), centrosomal tubulin, gamma 1 (TUBG1) (Supplementary Figure S3D), or endoplasmic reticulum protein disulfide isomerase, prolyl 4-hydroxylase, beta polypeptide (P4HB) (Supplementary Figure S3E).

We used mutant mice to determine whether the localization of EIF4G3 to the XY body was affected by the C-terminal *Eif4g3*$^{repro8}$ mutation. Localization of mutant EIF4G3 protein to the XY body was detected in spermatocytes from *Eif4g3*$^{repro8}$ mutant testes, suggesting that a fully functional C-terminal end of the protein is not required (Figure 3F). Moreover, there is XY body localization of EIF4G3 protein in spermatocytes of mice homozygous for a deletion of the testis-specific *Eif4g3* exon 5 (Figure 3G), indicating that this conserved N-terminal peptide is also not required for XY body localization. To determine if EIF4G3 (or its antibody) localizes nonspecifically, we investigated localization of EIF4G3 to the XY-like chromatin that is formed in the absence of DNA double-strand breaks (DSBs). Spermatocytes deficient for SPO11 meiotic protein covalently bound to DSB (SPO11), the protein inducing most meiotic DSBs, are characterized by a "pseudo-sex body" that labels with pH2AFX much like the XY body [35]. We analyzed *Spo11*$^{tm1Mjn}$*/J* mutant spermatocytes, and showed that EIF4G3 does not co-localize with the pH2AFX-labeled pseudo-sex body (Figure 3H). This correlates with other findings that markers of the mid-to late-pachytene XY body are not found on the pseudo-sex body of *Spo11* mutant spermatocytes [35,36]. Together, these observations suggest that EIF4G3 enrichment in the XY body occurs even in the absence of some critical domains of the EIF4G3 protein, is not associated with the dynamics of pH2AFX per se, and does not reflect nonspecific binding (of the protein or the antibody) to sex-body-like chromatin.

## Other translation initiation proteins as well as cell-cycle regulators are relatively enriched in the XY body

Because EIF4G3, but not EIF4G1, is enriched in the XY body, we determined the localization of other potentially interacting protein translation components in pachytene spermatocytes. Taken together, the proteins that we tested were each chosen because there is broad evidence for their participation in translation initiation and/or translation elongation; they encompass other members of the initiation complex, ribosomal subunit proteins, RBPs, and activators and repressors of translation. Many translational regulatory proteins tested exhibited some degree of enrichment in the XY body (Figure 4). These included EIF4F complex members (Figure 4A–D), ribosomal proteins (Figure 4E and F), RBPs musashi RNA-binding protein 1 (MSI1) and translin (TSN) (Figure 4G and H), translational activator MKNK family proteins MAP kinase-interacting serine/threonine kinase 1 and 2 (MKNK1 and MKNK2), which have been reported to activate EIF4E proteins by phosphorylation

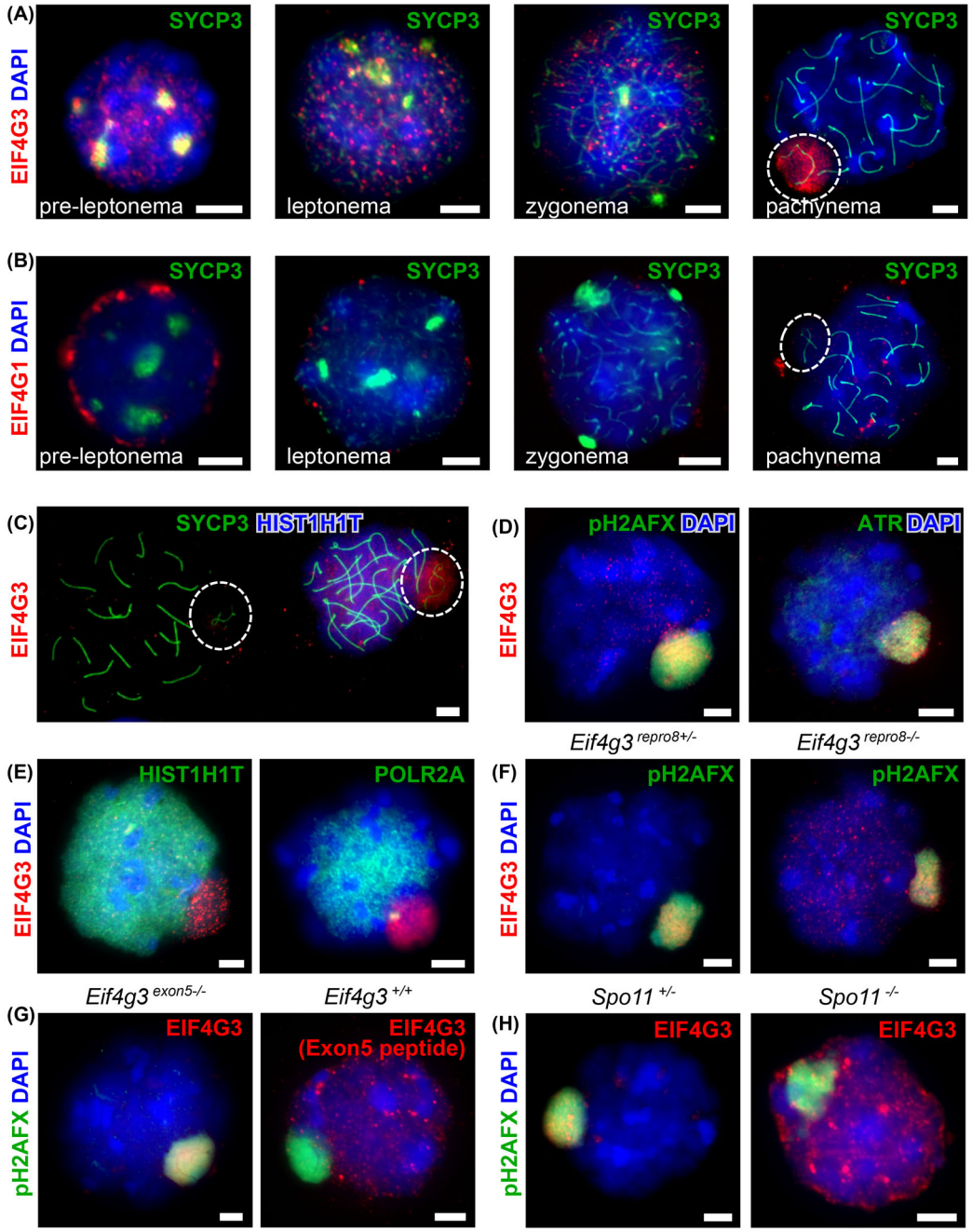


**Figure 3.** Immunofluorescence labeling of EIF4G3, EIF4G1, and meiotic prophase markers in spermatocytes. (**A**) EIF4G3 labeling in meiotic prophase cells also labeled with antibody to SYCP3 (synaptonemal complex protein) and DAPI (DNA) to identify meiotic prophase substages. EIF4G3 is highly enriched in the XY body (circled) during pachynema. (**B**) EIF4G1 labeling in meiotic prophase cells also labeled with antibody to SYCP3 and with DAPI. EIF4G1 is not reliably detected in the nucleus, or in the XY body (circled in far right panel). (**C**) Triple labeling of pachytene spermatocytes for EIF4G3, SYCP3, and HIST1H1T (histone H1t, a protein marker of mid-to-late pachynema). EIF4G3 is strong in mid-to-late pachytene spermatocytes (HIST1H1T high) and is negative or weak in early pachytene spermatocytes (HIST1H1T negative or weak). (**D**) Double labeling of pachytene spermatocytes for EIF4G3 and pH2AFX (phosphorylated histone H2AFX) and ATR (ATM-related protein), proteins known to localize to the XY body. (**E**) Double labeling of pachytene spermatocytes for EIF4G3 and HIST1H1T and POLR2A (RNA polymerase 2A), proteins known to not specifically localize to the XY body during pachynema. (**F**) Immunolabeling of EIF4G3 in late prophase spermatocytes isolated from *Eif4g3*$^{repro8/repro8}$ mutant and heterozygous testes. (**G**) Immunolabeling with anti-EIF4G3 (Bethyl) in late prophase spermatocytes isolated from *Eif4g3*$^{exon5/exon5}$ mutant lacking the conserved and testis-specific exon 5 and labeling of EIF4G3 in late prophase spermatocytes isolated from wild-type mice using the EIF4G3 exon5-specific antibody (Handel Lab/Thermo). (**H**) Co-immunolabeling of EIF4G3 and pH2AFX in *Spo11*$^{tm1Mjn}$*/J* heterozygous and mutant spermatocytes. Left: anti-EIF4G3 staining co-localizes with anti-pH2AFX in the XY body in late spermatocytes isolated from *Spo11*$^{tm1Mjn}$*/J* heterozygous. Right: anti-EIF4G3 staining is not co-localized with the pH2AFX-labeled pseudo-sex body or with any other domain in the *Spo11*$^{tm1Mjn}$*/J* mutant. Bars = 5 $\mu$m.

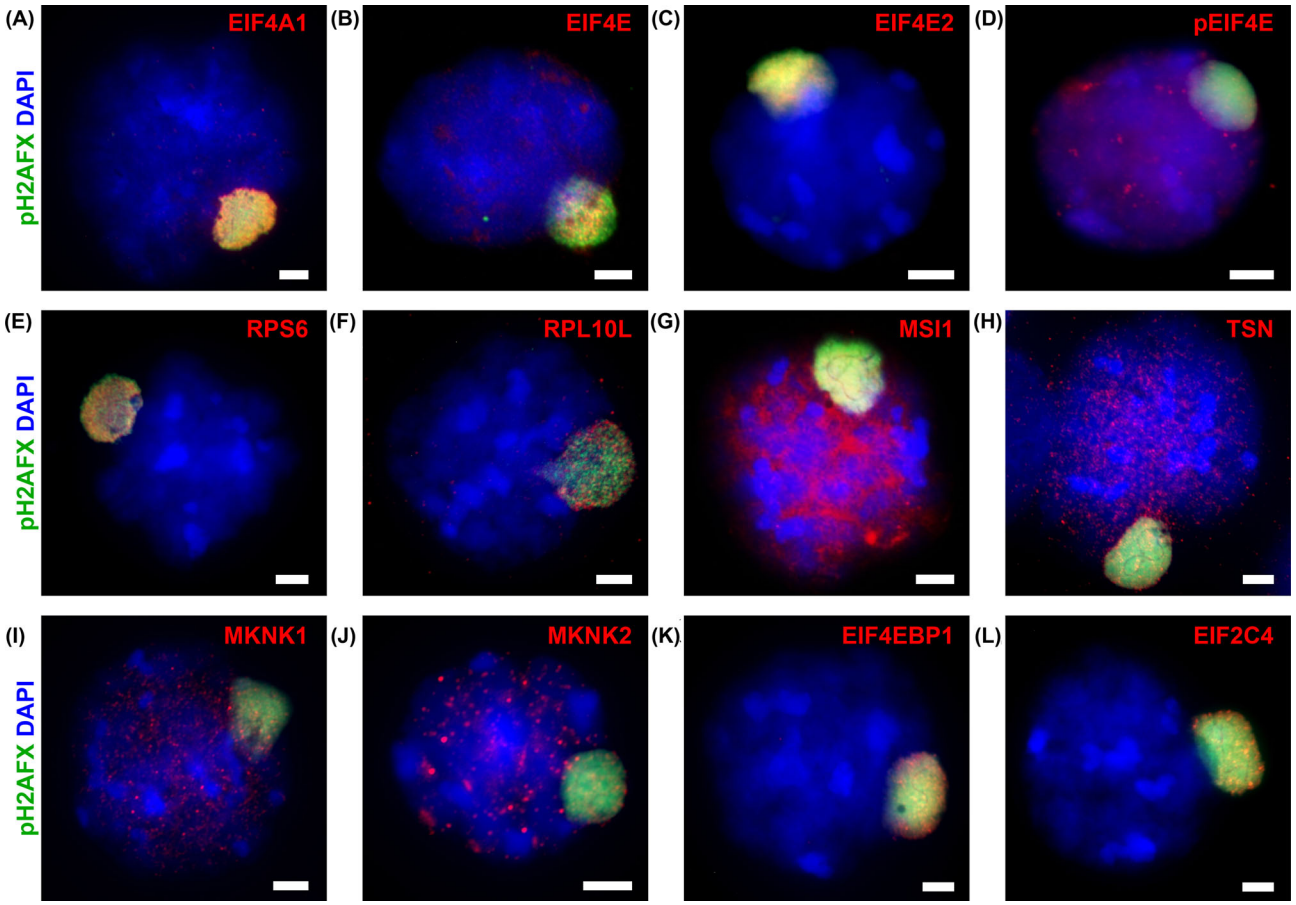


**Figure 4.** Some translational factors are relatively enriched in the XY body of pachytene spermatocytes. (**A-D**) EIF4F complex members EIF4A1, EIF4E, EIF4E2, and phosphorylated EIF4E were found in the XY body. (**E-H**) Small ribosomal subunit protein RPS6 and large ribosomal subunit protein RPL10L, and RNA-binding proteins MSI1 and TSN were relatively enriched in the XY body. (**I-L**) Translational activators MKNK1 and MKNK2, and repressors EIF4EBP1 and EIF2C4 (AGO4), were found in the XY body. Bars = 5 $\mu$m.

[37,38] (Figure 4I and J), and translational repressors, eukaryotic translation initiation factor 4E binding protein 1 (EIF4EBP1, also used as 4EBP1) (4EBP1) [39,40] and Argonaute RISC catalytic subunit 4 (AGO4) (EIF2C4) [41] (Figure 4K and L). Together, these observations present a picture of a diverse array of translation regulatory proteins unexpectedly enriched in a specific subnuclear domain, the XY body. However, it is not the case that all such translation-related proteins are present in the nucleus (Supplementary Figure S4). Many translation proteins tested were not present in the XY body; these included some members of the EIF4F complex, EIF4G2, EIF4A2, EIF4A3, and EIF4E3 (Supplementary Figure S4A), and small and large ribosomal subunit proteins ribosomal protein S3 (RPS3), ribosomal protein S13 (RPS13), ribosomal protein L10A (RPL10A), and ribosomal protein L28 (RPL28) (Supplementary Figure S4B). Interestingly, some RBPs that interact with EIF4G3 were also not detected in the XY body: boule homolog, RNA binding protein (BOLL) and ELAVL1 are localized in the nucleus, but not enriched in the XY body, while DAZL was not reliably detected in the nucleus (Supplementary Figure S4C).

Nonetheless, the accumulation of some translation initiation proteins in the XY body leads to the question of whether there is protein synthesis in nuclei of pachytene spermatocytes. It is challenging to detect subcellularly localized protein synthesis. One approach that has been used with success is to examine sites of puromycin incorporation. Puromycin, an inhibitor of translation, binds to actively translating ribosomes after a brief labeling period and stalls ongoing protein synthesis [27,28]; thus, subcellular sites of puromycin localization represent sites of translating ribosomes. We incubated pachytene spermatocytes with puromycin for 5 min, followed by collection of cells for surface-spread and whole-mount staining. In spread chromatin, although some anti-puromycin labeling was detected in the nucleus, it was not enriched in the XY body (Supplementary Figure S5A and B). In whole-mounted cells capturing three-dimensional nuclei, puromycin signal was strong in the cytoplasm, as expected, but considerably weaker in the nucleus (Supplementary Figure S5C). Thus, the puromycin assay did not provide strong evidence for active translation in the XY body. Because phosphorylated EIF4EBP1 plays important roles in promoting translation initiation through releasing EIF4E, its localization has also been used to detect subcellular sites of protein translation in oocytes [42]. Thus, we also examined spermatocytes with antibodies recognizing phosphorylated EIF4EBP1 on Ser64, Thr69, and Ser111. Antibody signals were detected in the nucleus, but none of them co-localized with pH2AFX or were enriched in the XY body (Supplementary Figure S5D–F). Taken together, these data provide no concrete evidence for ongoing protein translation in the XY body of spermatocytes.

Because the phenotype of the *Eif4g3*$^{repro8}$ mutation is arrest at the spermatocyte prophase-to-metaphase cell-cycle transition, and a known substrate of EIF4G3, *Hspa2* mRNA, encodes a

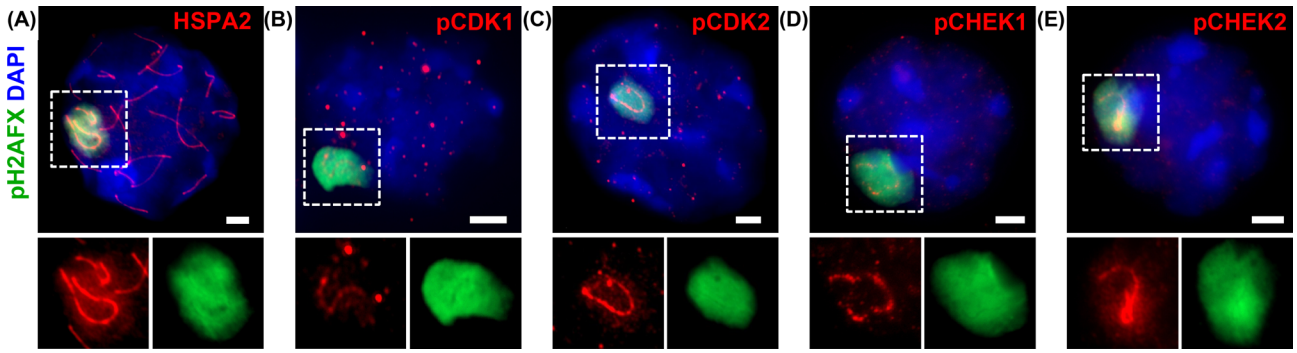


**Figure 5.** Relative enrichment of HSPA2 and cell-cycle regulators in the XY body. (**A**) HSPA2, a target of *Eif4g3*$^{repro8}$ mutant, was detected on chromosomal axes, including the X-Y axes, in spermatocyte nuclei. (**B-E**) Relative enrichment of cell-cycle regulators in the XY body. Phosphorylated CDK1, CDK2, CHEK1, and CHEK2 were all relatively enriched in the XY body and/or XY synaptonemal complex of spermatocytes. The boxed regions of these color-merged panels are shown in single color of red and green in the bottom row. Bars = 5 $\mu$m.

cell-cycle-related mediator of chromosome desynapsis [13,14], we considered the possibility that cell-cycle transition proteins might co-localize with EIF4G3 in the XY body. Results of immunolocalization analyses showed that HSPA2 was present as expected on both autosomal and the X and Y chromosomal axes in late prophase spermatocytes (Figure 5A). Phosphorylated cyclin-dependent kinase 1 (CDK1), cyclin-dependent kinase 2 (CDK2), checkpoint kinase 1 (CHEK1), and checkpoint kinase 1 (CHEK2) were also enriched in the XY body and/or on the XY synaptonemal complex axes in spermatocytes (Figure 5B–E). However, one caveat when considering the putative localization of phosphorylated proteins is that both the chromosome axes and the XY body are rich in phosphorylated proteins [43,44], which could lead to some antibodies raised against phosphorylated epitopes binding nonspecifically.

Taken together, these observations demonstrate that many components and activators of translation initiation complexes, as well as some cell-cycle regulatory proteins, are present in the nucleus and relatively enriched in the XY body of spermatocytes. However, because multiple small and large ribosomal subunit proteins are not similarly localized, and because ongoing protein synthesis cannot be detected, the XY body translation initiation complexes may not be fully constituted or translationally active.

## Discussion

All of the mammalian EIF4G translation factors (EIF4G1, EIF4G2, EIF4G3) are ubiquitous, but only the EIF4G3 variant has been shown to be required for spermatogenesis and male fertility in mice. A goal of this study was to define the differences in cellular dynamics between the canonical EIF4G1 and EIF4G3 proteins in spermatogenesis. During mid-to-late meiotic prophase, which is the phase arrested by mutation of *Eif4g3*, EIF4G1 is low and EIF4G3 is high. EIF4G1 exhibits, as expected, cytoplasmic localization throughout spermatogenesis. Most strikingly, EIF4G3 is predominantly in nuclei of spermatocytes, and highly enriched in the XY body, the chromatin domain containing the X and Y chromosomes. Moreover, other translation initiation factor proteins, ribosomal proteins, and RBPs are also present in the XY body. This highly specific localization for translation factors in spermatocytes is enigmatic; unraveling this requires consideration of possible roles for EIF4G3 and for the specificity of its localization to the XY body.

### Roles for EIF4G3

EIF4G is a well-studied member of the eukaryotic EIF4F translation initiation complex, where it plays an adaptor role. Its position in the translation initiation complex allows EIF4G proteins to position the mRNA transcript, by interacting with both PABP and with the 5′-cap, as well as bind several other essential initiation factors, most notably EIF4A, EIF4E, and EIF3. Together, these proteins scaffold interaction of mRNA and initiation factors onto the small subunit of the ribosome, allow recruitment of the large subunit, and give way to elongation factors after initiation of cap-dependent translation. In the testis, both EIF4G1 (the more common EIF4G protein) and EIF4G3 are present. Mutation of the *Eif4g3* gene, by either of two gene-trap mutation or by the *Eif4g3*$^{repro8}$ mutation, results in male infertility but no other apparent adverse phenotypes [20]. Thus, EIF4G3 must have unique function in spermatogenesis, and, in fact, we found previously that *Hspa2* mRNA fails to be translated efficiently when *Eif4g3* is mutated [20]. HSPA2 is a heat-shock chaperone protein that is required for male germ cells to exit meiotic prophase. Its function is to mediate the association of CDK and cyclin to form active MPF [13,14], and mutation of *Hspa2* phenocopies mutation of *Eif4g3*. Therefore, the meiotic arrest phenotype of spermatocytes with mutant *Eif4g3* is most likely due to the absence of HSPA2. However, this biologically reasonable conclusion begs several questions: Why EIF4G3 has a unique function in male germ cells, why its role cannot be executed by EIF4G1, and how EIF4G3 differs from EIF4G1. Together, these questions point to possible noncanonical roles for translation initiation factors.

There is evidence that EIF4G, as well as other eukaryotic translation initiation complex proteins, plays broader roles in RNA metabolism [21,45]. The initiation factor EIF4E may be involved in mRNA export from the nucleus, thus contributing to its oncogenic role [45]. Accumulating evidence suggests that EIF4G also may function in a variety of processes involved in the shepherding of mRNA from the site of its biogenesis in the nucleus to its translation in the cytoplasm. Nontranslation initiation nuclear functions proposed for EIF4G include roles in mRNA splicing and mRNA quality surveillance and degradation (nonsense-mediated decay, NMD). In yeast, EIF4G interacts with splicesome components and deletion of an isoform of EIF4G results in accumulation of unspliced transcripts [46]. EIF4G in mammalian cells interacts with RNA cap-binding proteins and members of the translation initiation complex to facilitate the pioneer round of translation that is associated with NMD; NMD

is inhibited by EIF4G cleavage [47], and these roles may be facilitated by the ability of EIF4G to provide a scaffold for recruitment of RBPs [21]. Together, these observations suggest possible nuclear functions for EIF4G3 and other translation proteins, and, in the future, single-cell or even subcellular transcriptomics may help resolve these possibilities.

### Nuclear localization of translation initiation factors

What might be the biological rationale for the specific subnuclear localization of EIF4G3 and other translation initiation factors to the XY body chromatin in the spermatocyte nucleus? First, EIF4G3 might function, either as a translation factor or in mRNA surveillance, in the XY body (a "spatial function" hypothesis). But alternatively, function of EIF4G3 in spermatocytes may be complete and it is degraded in the XY body (a "garbage dump" hypothesis). A third possibility is that EIF4G3 might be stored in the XY body, ready for future function (a "poising" hypothesis).

Localized translation is a well-known strategy for delivery of proteins where they are needed. One notable gametogenic example is the association of maternal RNA and EIF4EBPs with the spindle in mouse oocytes [42], but also the proteome of the mammalian spindle and midbody contains proteins related to translation and ribosomes [48,49]. Because the protein product of an mRNA substrate for EIF4G3, HSPA2, functions in the nucleus at the end of meiotic prophase, the idea of its local translation is biologically appealing. Expression of the *Hspa2* gene begins early in meiotic prophase [50,51] and HSPA2 protein is present in spermatocyte nuclei throughout much of meiotic prophase [50]. However, there is little evidence to support the hypothesis that EIF4G3 promotes active mRNA translation in the XY body. First, we found no convincing evidence for protein synthesis in the nucleus or XY body in the puromycin in situ assay. Second, the XY body is markedly depleted of mRNA, and because a variety of assays, including Cot-1 RNA-FISH to detect nascent RNA, show no evidence for ongoing transcription from the sex chromosomes [52,53], it is difficult to support a hypothesis that XY-localized EIF4G3 could be playing a direct nuclear mRNA surveillance role, such as facilitating splicing. Nonetheless, this consideration does not eliminate other possibilities, for example, a role in miRNA metabolism. It is known that the argonaute RISC catalytic subunit 2 (AGO2) binds to EIF4G1, thereby associating the cap-binding complex with miRNA metabolism involved in post-transcriptional gene silencing [54]. It is intriguing that in spermatocytes, AGO4 is localized in the XY body [41]. It has been proposed that miRNAs are not silenced in the XY body of spermatocytes [55,56], although the evidence is not clear [57]. Thus, a "spatial function" for translation factors in the XY body is an appealing hypothesis, but convincing validation will require functional assays that are of higher resolution and higher sensitivity than currently available.

The XY body, being largely inactive chromatin, may also attract or be a storage area for proteins to be directed to the proteasome, or otherwise eliminated. Because we found that EIF4G3 did not localize to the non-XY heterochromatic domain *Spo11* mutant spermatocytes, it does not appear to be the case that either the protein or antibody localizes to condensed chromatin in general. However, the XY body is a repository for many ubiquitinylated and sumoylated proteins [58–61]. Such protein marks could be functional, but can also target proteins for degradation, suggesting that the XY body could be a "garbage dump" for the nucleus. If so, these proteins may be assembled for release to cytoplasmic organelles for their degradation at the time of nuclear envelope breakdown at the onset of the meiotic division phase. This idea is not incompatible with special function of the marked proteins while in residence in the XY body. However, not only is the "garbage dump" hypothesis difficult to test, it also begs the question of why translation factors might be in the XY body in the first place.

The presence of many other translation initiation factors with EIF4G3 in the XY body, in spite of lack of robust evidence for ongoing protein synthesis, suggests other alternatives. The XY body may be a storage depot for surveillance, chaperoning, and assembling translation initiation complexes and other factors for spermiogenesis, poising them for immediate, and perhaps localized, action once the nuclear envelope breaks down at the meiotic division phase. It is particularly notable that cell-cycle regulators and both EIF4BP and the mRNA cap-binding protein EIF4E are enriched in the XY body. The 4E-BPs are important regulators of translation, negatively regulate assembly of EIF4E into the initiation complex, and are known to control localization of EIF4E [62]. Both EIF4BP and EIF4G compete to bind to EIF4E, with binding of EIF4BP inhibiting assembly of EIF4E into the initiation complex via its binding to EIF4G [63]. In somatic cells, these factors can be stored in the nucleus under stress, and then released to participate in translation. It is conceptually plausible that these factors are stored in the XY body of the spermatocyte nucleus, poised as a translational regulatory timing mechanism, to release and be activated when the nuclear membrane breaks down at the meiotic division phase. Such a "jump start" could facilitate the dramatic change in translational profile that occurs in spermatids [1,2,4]. This is particularly relevant with respect to potential transcripts from the X and Y chromosomes. Previous work [64] has shown them to be enriched for multicopy genes with postmeiotic expression. Possibly components of the translation machinery are localized to the XY body in order to ensure timely translation of critical spermiogenic proteins encoded on the sex chromosomes.

Overall, a "temporal poising" hypothesis seems most compatible with what is known about the required function and localization of EIF4G3 during meiosis. More specific information about the roster and extent of the specific mRNA clients for EIF4G3 and its cofactors, as well as the temporal and spatial dynamics of their localization, might enable proof of such a "poising" hypothesis. However, it is not currently possible to clearly delineate these mRNA substrates, due to the difficulty of separating EIF4G3 initiation complexes from the more abundant EIF4G1 complexes in testicular cells. Nonetheless, the localization of translation initiation factors to the XY chromatin domain of the spermatocyte nucleus suggests fascinating alternative functions for these translation factors as well as unexpected and yet-to-be resolved roles for the spermatocyte sex chromatin.

## Supplementary data

Supplementary data are available at *BIOLRE* online.

**Supplementary Figure S1.** Expression and localization of RNA-binding proteins during the first wave of spermatogenesis in mice. (**A**) Transcription of *Dazl*, *Elavl1*, and *Pabpc1* during the first wave of spermatogenesis. Total RNA was extracted from whole testes at age of 8–35 dpp. *Gapdh* was used as an internal control. These analyses were performed three times, with a representative result shown. (**B**) DAZL, ELAVL1, and PABPC1 protein expression was analyzed by western blots of whole testis protein extracts prepared from mice at 8–35 dpp. The loading control is tubulin, alpha 1A (TUBA1A). The second band on the DAZL blot may be degraded DAZL protein. The

second lower molecular weight band on the ELAVL1 blot is probably a second isoform of ELAVL1, since there is a known testis splicing variant. Molecular weight (kDa) positions are shown to the left of the blots in panels A and B. (**C**) Localization of DAZL, ELAVL1, and PABPC1 in germ cells during the first wave of spermatogenesis in mice. The testis histological sections were prepared from mice at 8–35 dpp, and immunolabeled with the same antibodies as used for western blotting. Bars = 40 $\mu$m.

**Supplementary Figure S2.** Test for specificity of EIF4G3 antibody. (**A**) Anti-EIF4G3 staining and EGFP are co-localized in HEK293 cells transfected with EIF4G3-EGFP. (**B**) Anti-EIF4G3 and anti-FLAG are co-localized in HEK293 cells transfected with EIF4G3-FLAG. (**C**) As a control, anti-EIF4G3 staining and DCP1A-RFP are not co-localized in HEK293 cells transfected with DCP1A-RFP (mRNA de-capping protein). Bars = 5 $\mu$m.

**Supplementary Figure S3.** Immunofluorescence labeling of EIF4G1 and EIF4G3 in whole-mount preparations. (**A**) EIF4G1 localizes to the cytoplasm, but is hardly detected in the nucleus, including the XY body. (**B**) EIF4G3 is highly enriched in the XY body and co-localizes with pH2AFX in the nucleus. (**C-E**) EIF4G3 is not highly enriched in the regions co-labeled for cytoplasmic mRNA processing P-body protein PIWIL2 (**C**), centrosomal gamma tubulin protein (TUBG1) (**D**), or endoplasmic reticulum protein disulfide isomerase, PDI (P4HB prolyl 4-hydroxylase, beta polypeptide) (**E**). Bars = 10 $\mu$m.

**Supplementary Figure S4.** Some translation regulators are not enriched in the XY body. (**A**) Members of EIF4F complex, such as EIF4G2, EIF4A2, EIF4A3, and EIF4E3, are not enriched in the XY body in spermatocytes. (**B**) Members of small and large unit ribosomal proteins, such as RPS3, RPS13, RPL10A, and RPL28 are not enriched in XY body of spermatocytes. (**C**) Immunostaining of RNA-binding proteins BOLL, DAZL, and ELAVL1. DAZL is not detected in the nucleus. Both BOLL and ELAVL1 are easily detected in the nucleus but neither is enriched in the XY body of spermatocytes. Bars = 5 $\mu$m.

**Supplementary Figure S5**. Detection of puromycin and phosphorylated EIF4EBP1 staining in late prophase spermatocytes**.** (**A, B**). Labeling of puromycin incorporated into pachytene spermatocytes was detected with monoclonal anti-puromycin, but not in ethanol-treated control spermatocytes. In surface-spread staining, puromycin can be detected in the nucleus, but the staining is not enriched in the XY body, which is labeled with pH2AFX (**C**). In whole-mount staining, anti-puromycin labeling is strong in the cytoplasm and weak in the nucleus. (**D-F**) Immunolabeling of late prophase spermatocytes with antibodies to EIF4EBP1phosphorylated on Ser64, Thr69, or Ser111. There is no enrichment of these phosphorylated EIF4EBP1 variants in the XY body compared to autosomal regions. Bar = 5 $\mu$m.

## Acknowledgments

We appreciate the assistance of Sabrina Petri and Catherine Brunton for expert maintenance of mouse colonies. We acknowledge the Scientific Services of the Jackson Laboratory for outstanding support, and Zoe Reifsnyder for assistance with figures. We thank Alicia Valenzuela and Drs. Beth Dumont and Aric Rogers for critical comments on the manuscript, and members of the Handel laboratory for many helpful discussions throughout this study.

## References

1. Chalmel F, Rolland AD, Niederhauser-Wiederkehr C, Chung SS, Demougin P, Gattiker A, Moore J, Patard JJ, Wolgemuth DJ, Jegou B, Primig M. The conserved transcriptome in human and rodent male gametogenesis. *Proc Natl Acad Sci USA* 2007; **104**:8346–8351.
2. Soumillon M, Necsulea A, Weier M, Brawand D, Zhang X, Gu H, Barthes P, Kokkinaki M, Nef S, Gnirke A, Dym M, de Massy B et al. Cellular source and mechanisms of high transcriptome complexity in the mammalian testis. *Cell Rep* 2013; **3**:2179–2190.
3. Ball RL, Fujiwara Y, Sun F, Hu J, Hibbs MA, Handel MA, Carter GW. Regulatory complexity revealed by integrated cytological and RNA-seq analyses of meiotic substages in mouse spermatocytes. *BMC Genomics* 2016; **17**:628.
4. da Cruz I, Rodriguez-Casuriaga R, Santinaque FF, Farias J, Curti G, Capoano CA, Folle GA, Benavente R, Sotelo-Silveira JR, Geisinger A. Transcriptome analysis of highly purified mouse spermatogenic cell populations: gene expression signatures switch from meiotic-to postmeiotic-related processes at pachytene stage. *BMC Genomics* 2016; **17**:294.
5. Braun RE. Temporal control of protein synthesis during spermatogenesis. *Int J Androl* 2000; **23**:92–94.
6. Hecht NB. Molecular mechanisms of male germ cell differentiation. *Bioessays* 1998; **20**:555–561.
7. Liu D, Brockman JM, Dass B, Hutchins LN, Singh P, McCarrey JR, MacDonald CC, Graber JH. Systematic variation in mRNA 3′-processing signals during mouse spermatogenesis. *Nucleic Acids Res* 2007; **35**:234–246.
8. Handel MA, Schimenti JC. Genetics of mammalian meiosis: regulation, dynamics and impact on fertility. *Nat Rev Genet* 2010; **11**:124–136.
9. Cobb J, Cargile B, Handel MA. Acquisition of competence to condense metaphase I chromosomes during spermatogenesis. *Dev Biol* 1999; **205**:49–64.
10. Handel MA, Cobb J, Eaker S. What are the spermatocyte's requirements for successful meiotic division? *J Exp Zool* 1999; **285**:243–250.
11. Sun F, Handel MA. Regulation of the meiotic prophase I to metaphase I transition in mouse spermatocytes. *Chromosoma* 2008; **117**:471–485.
12. Jordan P, Handel MA. *Inhibition of Polo-Like Kinase 1 Activity Prevents Synaptonemal Complex Disassembly*. North American Testis Workshop. Montreal, Canada; 2011.
13. Dix DJ, Allen JW, Collins BW, Poorman-Allen P, Mori C, Blizard DR, Brown PR, Goulding EH, Strong BD, Eddy EM. HSP70-2 is required for desynapsis of synaptonemal complexes during meiotic prophase in juvenile and adult mouse spermatocytes. *Development* 1997; **124**: 4595–4603.
14. Zhu DH, Dix DJ, Eddy EM. HSP70-2 is required for CDC2 kinase activity in meiosis I of mouse spermatocytes. *Development* 1997; **124**:3007–3014.
15. Franklin-Dumont TM, Chatterjee C, Wasserman SA, Dinardo S. A novel eIF4G homolog, Off-schedule, couples translational control to meiosis and differentiation in *Drosophila* spermatocytes. *Development* 2007; **134**:2851–2861.
16. Baker CC, Fuller MT. Translational control of meiotic cell cycle progression and spermatid differentiation in male germ cells by a novel eIF4G homolog. *Development* 2007; **134**:2863–2869.
17. Amiri A, Kelper BD, Kawasaki I, Fan Y, Kohara Y, Rhoads RE, Strome S. An isoform of eIF4E is a component of germ granules and is required for spermatogenesis in *C. elegans*. *Development* 2001; **128**:3899–3912.
18. Rhoads RE. eIF4E: new family members, new binding partners, new roles. *J Biol Chem* 2009; **284**:16711–16715.
19. Song A, Labella S, Korneeva NL, Keiper BD, Aamodt EJ, Zetka M, Rhoads RE. A *C. elegans* eIF4E-family member upregulates translation at elevated temperatures of mRNAs encoding MSH-5 and other meiotic crossover proteins. *J Cell Sci* 2010; **123**:2228–2237.
20. Sun F, Palmer K, Handel MA. Mutation of *Eif4g3*, encoding a eukaryotic translation initiation factor, causes male infertility and meiotic arrest of mouse spermatocytes. *Development* 2010; **137**:1699–1707.
21. Das S, Das B. eIF4G-an integrator of mRNA metabolism? *FEMS Yeast Res* 2016; **16**. doi:10.1093/femsyr/fow087.
22. Handel MA. The XY body: A specialized meiotic chromatin domain. *Exp Cell Res* 2004; **296**:57–63.
23. Turner JM. Meiotic sex chromosome inactivation. *Development* 2007; **134**:1823–1831.
24. La Salle S, Sun F, Handel MA. Isolation and short-term culture of mouse spermatocytes for analysis of meiosis. In: Keeney S (ed.) *Methods in Molecular Biology, Molecular Medicine and Biotechnology: Meiosis Protocols*, vol. 558: Springer, New York City, NY: Humana Press; 2009: 279–297.

25. Cobb J, Reddy RK, Park C, Handel MA. Analysis of expression and function of topoisomerase I and II during meiosis in male mice. *Mol Reprod Dev* 1997; **46**:489–498.
26. Cobb J, Miyaike M, Kikuchi A, Handel MA. Meiotic events at the centromeric heterochromatin: histone H3 phosphorylation, topoisomerase II alpha localization and chromosome condensation. *Chromosoma* 1999; **108**:412–425.
27. David A, Dolan BP, Hickman HD, Knowlton JJ, Clavarino G, Pierre P, Bennink JR, Yewdell JW. Nuclear translation visualized by ribosome-bound nascent chain puromycylation. *J Cell Biol* 2012; **197**:45–57.
28. Liu J, Xu Y, Stoleru D, Salic A. Imaging protein synthesis in cells and tissues with an alkyne analog of puromycin. *Proc Natl Acad Sci USA* 2012; **109**:413–418.
29. Bustin SA. Absolute quantification of mRNA using real-time reverse transcription polymerase chain reaction assays. *J Mol Endocrinol* 2000; **25**:169–193.
30. Tcherkezian J, Cargnello M, Romeo Y, Huttlin EL, Lavoie G, Gygi SP, Roux PP. Proteomic analysis of cap-dependent translation identifies LARP1 as a key regulator of 5'TOP mRNA translation. *Genes Dev* 2014; **28**:357–371.
31. Ruggiu M, Speed R, Taggart M, McKay SJ, Kilanowski F, Saunders P, Dorin J, Cooke HJ. The mouse Dazla gene encodes a cytoplasmic protein essential for gametogenesis. *Nature* 1997; **389**:73–77.
32. Nguyen Chi M, Auriol J, Jegou B, Kontoyiannis DL, Turner JM, de Rooij D, Morello D. The RNA-binding protein ELAVL1/HuR is essential for mouse spermatogenesis, acting both at meiotic and postmeiotic stages. *Mol Biol Cell* 2011; **22**:2875–2885.
33. Kimura M, Ishida K, Kashiwabara S, Baba T. Characterization of two cytoplasmic poly(A)-binding proteins, PABPC1 and PABPC2, in mouse spermatogenic cells. *Biol Reprod* 2009; **80**:545–554.
34. Inselman A, Eaker S, Handel MA. Temporal expression of cell cycle-related proteins during spermatogenesis: establishing a timeline for onset of the meiotic divisions. *Cytogenet Genome Res* 2003; **103**:277–284.
35. Bellani MA, Romanienko PJ, Cairatti DA, Camerini-Otero RD. SPO11 is required for sex-body formation, and Spo11 heterozygosity rescues the prophase arrest of Atm-/- spermatocytes. *J Cell Sci* 2005; **118**:3233–3245.
36. Barchi M, Mahadevaiah S, Di Giacomo M, Baudat F, de Rooij DG, Burgoyne PS, Jasin M, Keeney S. Surveillance of different recombination defects in mouse spermatocytes yields distinct responses despite elimination at an identical developmental stage. *Mol Cell Biol* 2005; **25**:7203–7215.
37. Waskiewicz AJ, Johnson JC, Penn B, Mahalingam M, Kimball SR, Cooper JA. Phosphorylation of the cap-binding protein eukaryotic translation initiation factor 4E by protein kinase Mnk1 in vivo. *Mol Cell Biol* 1999; **19**:1871–1880.
38. Ueda T, Watanabe-Fukunaga R, Fukuyama H, Nagata S, Fukunaga R. Mnk2 and Mnk1 are essential for constitutive and inducible phosphorylation of eukaryotic initiation factor 4E but not for cell growth or development. *Mol Cell Biol* 2004; **24**:6539–6549.
39. Richter JD, Sonenberg N. Regulation of cap-dependent translation by eIF4E inhibitory proteins. *Nature* 2005; **433**:477–480.
40. Gingras AC, Raught B, Gygi SP, Niedzwiecka A, Miron M, Burley SK, Polakiewicz RD, Wyslouch-Cieszynska A, Aebersold R, Sonenberg N. Hierarchical phosphorylation of the translation inhibitor 4E-BP1. *Genes Dev* 2001; **15**:2852–2864.
41. Modzelewski AJ, Holmes RJ, Hilz S, Grimson A, Cohen PE. AGO4 regulates entry into meiosis and influences silencing of sex chromosomes in the male mouse germline. *Dev Cell* 2012; **23**:251–264.
42. Romasko EJ, Amarnath D, Midic U, Latham KE. Association of maternal mRNA and phosphorylated EIF4EBP1 variants with the spindle in mouse oocytes: localized translational control supporting female meiosis in mammals. *Genetics* 2013; **195**:349–358.
43. Fukuda T, Pratto F, Schimenti JC, Turner JM, Camerini-Otero RD, Hoog C. Phosphorylation of chromosome core components may serve as axis marks for the status of chromosomal events during mammalian meiosis. *PLoS Genet* 2012; **8**:e1002485.
44. Fedoriw AM, Menon D, Kim Y, Mu W, Magnuson T. Key mediators of somatic ATR signaling localize to unpaired chromosomes in spermatocytes. *Development* 2015; **142**:2972–2980.
45. Osborne MJ, Borden KL. The eukaryotic translation initiation factor eIF4E in the nucleus: taking the road less traveled. *Immunol Rev* 2015; **263**:210–223.
46. Kafasla P, Barrass JD, Thompson E, Fromont-Racine M, Jacquier A, Beggs JD, Lewis J. Interaction of yeast eIF4G with spliceosome components: implications in pre-mRNA processing events. *RNA Biol* 2009; **6**:563–574.
47. Lejeune F, Ranganathan AC, Maquat LE. eIF4G is required for the pioneer round of translation in mammalian cells. *Nat Struct Mol Biol* 2004; **11**:992–1000.
48. Skop AR, Liu H, Yates J 3rd, Meyer BJ, Heald R. Dissection of the mammalian midbody proteome reveals conserved cytokinesis mechanisms. *Science* 2004; **305**:61–66.
49. Bonner MK, Poole DS, Xu T, Sarkeshik A, Yates JR, 3rd Skop AR. Mitotic spindle proteomics in Chinese hamster ovary cells. *PLoS One* 2011; **6**:e20489.
50. Allen JW, Dix DJ, Collins BW, Merrick BA, He C, Selkirk JK, Poorman-Allen P, Dresser ME, Eddy EM. HSP70-2 is part of the synaptonemal complex in mouse and hamster spermatocytes. *Chromosoma* 1996; **104**:414–421.
51. Inselman AL, Nakamuro N, Brown PR, Willis WD, Goulding EH, Eddy EM. Heat shock protein 2 promoter drives Cre expression in spermatocytes of transgenic mice. *Genesis* 2010; **48**:114–120.
52. Namekawa SH, Park PJ, Zhang LF, Shima JE, McCarrey JR, Griswold MD, Lee JT. Postmeiotic sex chromatin in the male germline of mice. *Curr Biol* 2006; **16**:660–667.
53. Turner JMA, Mahadevaiah SK, Fernandez-Capetillo O, Nussenzweig A, Xu X, Deng C-X, Burgoyne PS. Silencing of unsynapsed meiotic chromosomes in the mouse. *Nat Genet* 2005; **37**:41–47.
54. Ryu I, Park JH, An S, Kwon OS, Jang SK. eIF4GI facilitates the microRNA-mediated gene silencing. *PLoS One* 2013; **8**:e55725.
55. Sosa E, Flores L, Yan W, McCarrey JR. Escape of X-linked miRNA genes from meiotic sex chromosome inactivation. *Development* 2015; **142**:3791–3800.
56. Song R, Ro S, Michaels JD, Park C, McCarrey JR, Yan W. Many X-linked microRNAs escape meiotic sex chromosome inactivation. *Nat Genet* 2009; **41**:488–493.
57. Royo H, Seitz H, ElInati E, Peters AH, Stadler MB, Turner JM. Silencing of X-linked microRNAs by meiotic sex chromosome inactivation. *PLoS Genet* 2015; **11**:e1005461.
58. Rogers RS, Inselman A, Handel MA, Matunis MJ. SUMO modified proteins localize to the XY body of pachytene spermatocytes. *Chromosoma* 2004; **113**:233–243.
59. La Salle S, Sun F, Zhang XD, Matunis MJ, Handel MA. Developmental control of sumoylation pathway proteins in mouse male germ cells. *Dev Biol* 2008; **321**:227–237.
60. Vigodner M, Morris PL. Testicular expression of small ubiquitin-related modifier-1 (SUMO-1) supports multiple roles in spermatogenesis: Silencing of sex chromosomes in spermatocytes, spermatid microtubule nucleation, and nuclear reshaping. *Dev Biol* 2005; **282**:480–492.
61. Vigodner M. Sumoylation precedes accumulation of phosphorylated H2AX on sex chromosomes during their meiotic inactivation. *Chromosome Res* 2009; **17**:37–45.
62. Rong L, Livingstone M, Sukarieh R, Petroulakis E, Gingras AC, Crosby K, Smith B, Polakiewicz RD, Pelletier J, Ferraiuolo MA, Sonenberg N. Control of eIF4E cellular localization by eIF4E-binding proteins, 4E-BPs. *RNA* 2008; **14**:1318–1327.
63. Schmidt C, Beilsten-Edmands V, Robinson CV. Insights into eukaryotic translation initiation from mass spectrometry of macromolecular protein assemblies. *J Mol Biol* 2016; **428**:344–356.
64. Mueller JL, Mahadevaiah SK, Park PJ, Warburton PE, Page DC, Turner JM. The mouse X chromosome is enriched for multicopy testis genes showing postmeiotic expression. *Nat Genet* 2008; **40**:794–799.